

DESIGN CONSIDERATIONS OF HIGH PEAK POWER GYROKLYSTRONS
FOR LINEAR COLLIDERS*

W. Lawson, P.E. Latham, J. Calame, M. Skopec, D. Welsh, B. Hogan, W. Wang, M.E. Read[†],
C.D. Striffler, M. Reiser, and V.L. Granatstein
Laboratory for Plasma Research
University Maryland, College Park, MD 20742

ABSTRACT

In this paper, the final preparations for bringing the University of Maryland's 10 GHz, 30 MW gyrokystron experiment on-line are discussed. We explain the enhanced circuit modelling and present a two cavity design which predicts an efficiency of 33% and a gain of 27 dB with the simulated beam parameters. We describe initial operation of the modulator and electron gun and detail the experimental design of the system. Finally, we present plans for a high gain gyrokystron circuit and discuss scaling considerations for producing powers in excess of 100 MW in the frequency range 10-30 GHz.

INTRODUCTION

The results of scaling studies for the next generation of linear electron-positron colliders have demonstrated a need for high pulse power, high efficiency, high gain microwave (8-30 GHz) amplifiers.¹ As part of our investigation into the suitability of gyrotron amplifiers for this application, we are constructing an X-band gyrokystron which is predicted to achieve a peak power of 30-50 MW.² Successful operation of this device will increase the state-of-the-art in gyrokystron power capability by three orders of magnitude and will establish the gyrokystron as a viable candidate to drive high-energy linear colliders.

A schematic of the major subsystems of the initial two-cavity gyrokystron is shown in Fig. 1. The modulator supplies a 500 kV, 200 A, 1.5 μ s pulse with an intermediate voltage to a double-anode Magnetron Injection Gun (MIG). The MIG generates a rotating beam which passes through the circuit after being adiabatically compressed. The beam's phase-space distribution is modulated by a microwave signal which is injected into the first cavity. Energy is extracted axially through a coupling aperture in the second cavity and travels through a nonlinear waveguide to a half-wavelength output window. The beam expands in the decreasing magnetic field and impinges on a 35 cm section of the output waveguide. A directional coupler and water calorimeter (not shown) measure the peak and average microwave power. The nominal parameters of this configuration are listed in Table I and details of these subsystems are discussed below.

ELECTRON BEAM GENERATION

The 500 kV voltage pulse is generated by an 8-12 stage line-type modulator. Four pulse-forming networks (PFNs) in parallel are resonantly charged on command to 46 kV and are switched through two thyratrons into a 1:22 pulse transformer which provides the required potential of 500 kV. The electron gun is in the double anode MIG configuration.³ Key dimensions of the gun design are listed in Table II and the simulated beam properties at 160 A are listed in Table I. The gun has been constructed by Varian Associates⁴ and has passed its ac-

ceptance test. A 1 μ s, 500 kV pulse was applied to the MIG when the cathode was cold. The voltage pulse and charging current are shown in Fig. 2. Without the axial magnetic field, a 143 kV pulse was applied with the cathode hot ($\sim 950^\circ\text{C}$) and the control anode grounded. The resulting 120 A pulse represents a current density of 4.2 A/cm² and is shown in Fig. 3. The current was limited by the impedance of the modulator. Preparations are being made to draw the full power beam.

MICROWAVE CIRCUIT

To design the microwave circuits, we use a partially self-consistent steady state, numerical code⁵ that has evolved considerably during the past three years. The cold cavity field profiles are found from a scattering matrix formulation.⁶ The effect of ac space-charge waves has been incorporated both as a frequency shift and a perturbation on the perpendicular field profile. The parameters of the two cavity design are listed in Table I along with the simulated results. The low Q of the input cavity is realized by two thin, carbon-impregnated aluminosilicate annuli located on either cavity end at the outer radius. Cold tests have revealed that we can achieve the required frequency and Q with such absorbers. The scattering matrix code was modified to include lossy dielectrics and was successfully compared to analytic results in simple geometries with lossy dielectrics and numeric codes (mafia and urnel-t) for complex geometries with loss-free dielectrics. This code also predicts the viability of the lossy rings.

A linear start oscillation code based on the scattering matrix formulation predicts that an all metal drift tube will have no stable region of operation. To suppress the unwanted modes, a drift tube consisting of alternate washers of metal and lossy dielectric will be used. Again, both experimental and analytic results indicate the viability of this technique. Our first tube will utilize six rings of MgO with a 1% concentration of SiC. The dielectric rings are 22% wider than the alternating metal rings and have a depth of 1.6 cm. The drift tube provides 117 dB isolation for the TE₀₁ mode and more than 16 dB isolation for the uncut-off modes at 10 GHz.

The output cavity Q is essentially diffractive and is sufficiently larger than the minimum Q so that a simple coupling iris can be used for the endfire system. Cold testing has confirmed both the frequency and Q predicted by the scattering matrix code for a variety of configurations.

The vacuum vessel between the output cavity and the output window doubles as the microwave and beam transport system and is shown in Fig. 6. A nonlinear taper brings the waveguide radius from 2.60 cm to the beam dump radius of 3.57 cm in 19.5 cm. The smaller radius can support only the lowest circular electric mode (TE₀₁) at 10 GHz while the larger radius can support the lowest two circular modes. To minimize mode conversion, a raised cosine radius is used. An approximate analytic solution predicts the mode conversion to be less than 1.1×10^4 percent in power.

Computer simulations of the beam with and without microwave interaction show that the beam is dumped fairly uni-

*Work supported by U.S. Department of Energy.

† Physical Sciences, Inc., Alexandria, VA.

formly by the decaying magnetic field over a 35 cm distance in the beam dump. This keeps the instantaneous temperature rise below 20° and the average temperature rise sufficiently low to allow modest water cooling. A dumping magnet prevents the few high energy electrons from reaching the output window. The vacuum port consists of a stainless steel tube with 150 holes distributed uniformly in angle and axial position to provide sufficient conductance with minimal microwave interference.

A second nonlinear taper is used after the beam dump to bring the radius to 6.35 cm. At that radius, four circular electric modes can propagate, but the ideal mode conversion to all other modes is still less than 0.002 percent in power. A half wavelength BeO window, brazed to a stainless steel flange via a Kovar ring, provides the vacuum-to-air interface.

DIAGNOSTICS

There will be several standard external current transformers in conjunction with current breaks to measure the instantaneous beam current at several locations along the system. Capacitive probes, which consist of four 90° sections and a sapphire insulator, will be used at several locations in an initial beam test to measure total beam density and relative location. The two diagnostics jointly will give an estimate of the average axial velocity and (along with the beam voltage) will provide information about the average velocity ratio.

The microwave diagnostics consist of both peak and average power measurements. The peak power measurement involves a mode selective directional coupler combined with a crystal detector. Because the circular guide is highly overmoded and the rectangular guide is not, the phase velocity of the two waves cannot be the same and two sets of coupling holes are required. The 50 dB, TE₀₁⁰ → TE₁₀⁰ coupler is designed to maximize TE₀₁⁰ directivity (-83 dB) and minimize TE₁₁⁰ coupling (-75 dB). The detector will provide the signal envelope and, with proper calibration, an estimate of the peak power. A non-resonant water calorimeter will provide the average power measurement and a check of the peak power measurement. Water is circulated between two 19.5 cm long styrcast cones to maximize sensitivity. The thickness is adjusted to guarantee a minimum attenuation of 28 dB.

SCALED DESIGNS

To achieve high gain, high efficiency gyrokystrons, multicavity circuits will be utilized. Simulations of a four cavity design with 4.5 cm long drift tubes and two buncher cavities with the approximate dimensions of the input cavity indicate that an efficiency of 45% and a large signal gain of 63 dB is achievable with the simulated beam parameters.

To achieve significantly higher power levels, the circuit will have to be modified considerably. The current limitation is the peak power capability of the magnetron injection gun. Scaling laws have been derived⁷ which predict the dependence of the beam power on beam voltage, peak applied electric field, and the beam radius (related to cavity mode). If $\gamma_0 = 1 + V_0/(mc^2)$ is the normalized beam energy, E_m is the maximum electric field, and r_g is the average beam radius, then the peak power P_0 scales as follows:

$$P_0 \propto (\gamma_0 - 1)^2 (1 + \gamma_0^{-1}) E_m r_g. \quad (1)$$

From this relation we have designed a gun for a coaxial cavity (with twice the beam radius) at an energy of 800 keV which should be capable of producing 180 MW of 10 GHz microwave

power.¹ Further power increases would be possible if we were to relax the constraint on maximum electric field which is currently $E_m < 90$ kV/cm.

To achieve high frequencies, again the trade-off between power and frequency in the gun is fundamental. The MIG frequency scaling is $P_0 \alpha f^{-1}$, which is superior to pierce gun scaling when considering high frequencies. This scaling has been confirmed with numerical simulations and should make the gyrokystron an even stronger contender to power the linear supercollider if the proposed operating frequency exceeds 10 GHz.

REFERENCES

1. M. Reiser, D. Chernin, W. Lawson, and A. Mondelli, 3rd Workshop of the INFN Eloisatron Project, Erice, Italy, May 1987.
2. K.R. Chu, V.L. Granatstein, P.E. Latham, W. Lawson, and C.D. Striffler, IEEE Trans. Plasma Sci., PS-13, pp. 424-434, 1985.
3. W. Lawson, J. Calame, V.L. Granatstein, G.S. Park, C.D. Striffler, and J. Neilson, Int. J. Electronics, 61, pp. 969-984, 1986.
4. R.F. Garcia, K.L. Felch, Y.M. Mizuhara, S.T. Spang, and W. Lawson, 1987 IEDM Tech. Digest, p. 821.
5. K.R. Chu, V.L. Granatstein, P.E. Latham, W. Lawson, and C.D. Striffler, IEEE Trans. Plasma Sci., PS-13, p. 424 (1985).
6. J. Neilson, P.E. Latham, M. Caplan, W. Lawson, submitted to IEEE Trans. Microwave Theory Tech., August, 1988.
7. W. Lawson, IEEE Trans. Plasma Sci. 16, pp. 290-295 (1988).

Table I.
The Two Cavity Gyrokystron Parameters.

Beam	Power P_0	80 MW
	Voltage V_0	500 kV
	Velocity ratio v_{\perp}/v_z	1.5
	Velocity spread Δv_z	7.0%
	Larmor radius r_L	0.43 cm
	Center radius r_g	0.79 cm
	Guiding spread Δr_g	0.20 cm
Circuit	Axial field B_0	0.565 T
	Mode (both cavities)	TE ₀₁₁
	Peak Efficiency	33%
Input Cavity	Gain	27 dB
	Radius	4.50 cm
	Length	1.53 cm
	Q	225
Drift Tube	Injected Power	50 kW
	Radius	1.50 cm
	Length	9.00 cm
Output Cavity	Radius	2.11 cm
	Length	2.38 cm
	Q	165
Aperture	Radius	1.50 cm
	Length	0.33 cm
Output Guide	Radius	2.60 cm

Table II.
80 MW MIG Electrode Specifications.

Cathode Radius r_c	0.0228 m
Emitter Strip Width ℓ_s	0.020 m
Cathode-Control Anode Gap d_{ac}	0.0613 m
Cathode Half Angle ϕ_c	20°
Compression Ratio f_m	12
Control Anode Voltage V_a	143 kV
Emission Current Density J_c (Uniform)	5.61 A/cm ²

GYROKLYSTRON SCHEMATIC

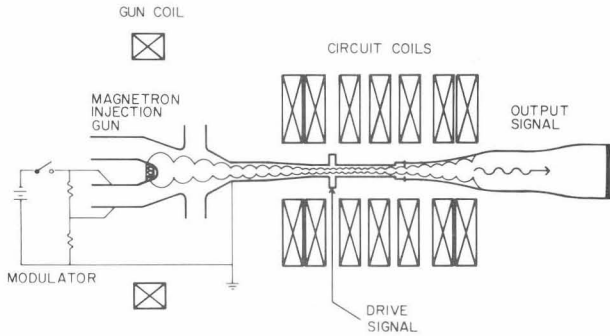


Figure 1.
The University of Maryland 30 MW Gyrokystron.

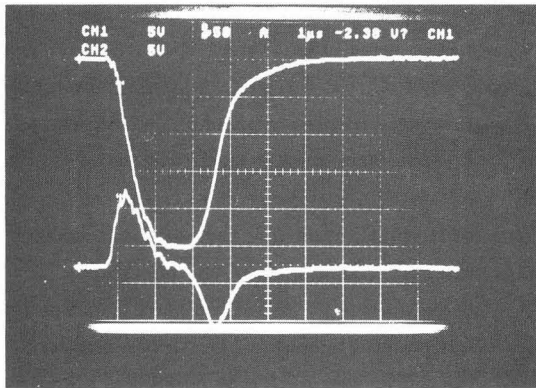


Figure 2.

A typical modulator pulse. The upper trace shows the voltage pulse with 100 kV/div. The lower trace shows the charging current with 50 A/div. The sweep rate is 1 μs/div.

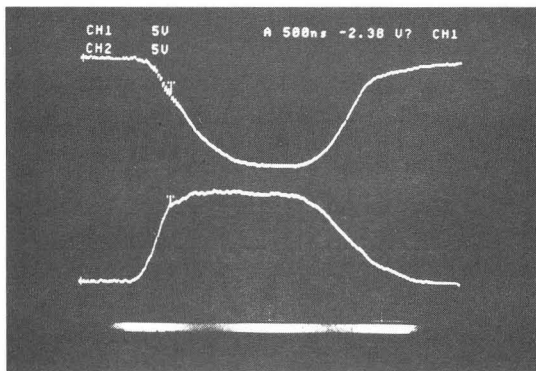


Figure 3.

The current pulse. The upper trace shows the voltage pulse in 50 kV/div and the lower trace shows the current pulse in 50 A/div. The sweep rate is 500 ns/div.